

## MAGNETIC SUSPENSION SYSTEM WITH PERMANENT MAGNET MOTION CONTROL

**Koichi Oka**

University of Tokyo, Tokyo, Japan

**Toshiro Higuchi**

University of Tokyo, Tokyo, Japan

Kanagawa Academy of Scientific Technology, Kawasaki, Kanagawa

### ABSTRACT

A novel active mag-lev system, featuring a bearing force control method, is being developed. In conventional systems, bearing force is controlled by an electrical method in which electromagnet coil currents are varied. However, in the proposed system, bearing force is controlled by a mechanical method in which the air gap between a permanent magnet and the levitated object is varied. As permanent magnets are used, the proposed system is effective for eliminating heat generation and saving energy.

First, the principle of this suspension system is explained. Next, a 1 DOF ball suspension system based on the proposed concept is introduced. Theoretical analyses of this system prove the feasibility of non-contact suspension and self-sensing controller. Experimental examinations support the analyses well. Additionally, a separate 3 DOF disk suspension system is discussed and analyzed from a control method point view, and another system employing a piezoelectric actuation element and self-sensing controller has been considered. Finally the concept of using electrostatics, in place of permanent magnets as an attractive force means is introduced.

### INTRODUCTION

There are many kinds of mag-lev systems[1][2]. Static levitation systems without superconductors need feedback loops and control of magnetic forces. Position sensors and electromagnets with current feedback control are usually used in electromagnetic suspension (EMS) systems. Position sensors sense the movement of suspended object, and magnetic forces are actively controlled by the electromagnet coil currents determined based on the sensor signals. However, electromagnet coils sometimes cause a heat generation problem.

Thus, We propose novel active mag-lev system with permanent magnets and a motion control mechanism in place of electromagnets and a current control mechanism. Owing to the use of permanent magnets, the merits of this system are that it eliminates problematic heat generation and is effective for saving energy. Also, with the application of this concept, a non-contact bearing mechanism can be added to systems such as conveyers, which already possess motion control schemes, through the installation of permanent magnets only.

In this paper, we explain the principle of the proposed magnetic suspension system, describe theoretical and experimental examinations of two types of suspension system, and consider various non-contact suspension system based on the proposed concept.

### PRINCIPLE OF THE PROPOSED MAG-LEV SYSTEM

An outline of one typical proposed system is shown in Figure 1. A ferromagnetic body is levitated by the attractive force from a permanent magnet positioned above. The magnet is driven by an actuator. The direction of levitation is vertical, and the magnet and the object move only in this direction. The equilibrium position is balanced by the gravity force and the magnet force.

If the actuator does not actively control the magnet's position, the levitated object will either fall or adhere to the magnet. Servo-control of the actuator make this system stable. Because there is a smaller attractive force for a larger air gap between the permanent magnet and object, the actuator drives the magnet upwards in response to object movement from its equilibrium position towards the magnet. Similarly, the actuator drives the magnet downwards in response to object movement away from the magnet. In this way, the object can be stably suspended without contact.

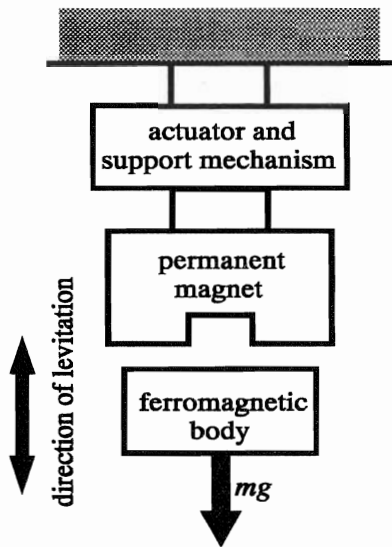


FIGURE 1: Magnetic Suspension System with Permanent Magnet Motion Control

In comparison to the electrical control method of EMS systems, this system is a mechanical control mag-lev system

### 1 DOF MAGNETIC SUSPENSION SYSTEM

To prove the feasibility of the proposed system, a 1 DOF experimental system was constructed as shown in the Figure 2, and its photograph is shown in Figure 3. A voice coil motor (VCM) is employed as the actuator of the permanent magnet. The shaded components in the figure move in concert with the permanent magnet and are supported by parallel plate springs. The shape of the permanent magnet is cylindrical 10 mm diameter and 4 mm height, with its magnetic poles aligned in the vertical direction. The suspended object is an iron ball with 19 mm diameter. The position of the ball is sensed by an eddy current gap sensor located under the ball. The resolution of the sensor is 0.5  $\mu\text{m}$ . The control system has a PD feedback loop and drives the VCM via a voltage amplifier.

In this system, the vertical direction of movement of the ball is controlled actively, while the other DOFs are stable without active control. In horizontal translational movements, the potential forces act the ball to be positioned under the magnet, and the effect of residual magnetism of the ball settles the configuration about the rotation. The movements of these 5 DOFs are damped by the effect of air viscosity and eddy current.

### Symbols and Parameters

Symbols and parameters in 1 DOF suspension system are:

$k_e$  = spring constant of parallel plate spring (4.57 kN/m)  
 $\xi$  = damping factor of spring (0.27 Ns/m)

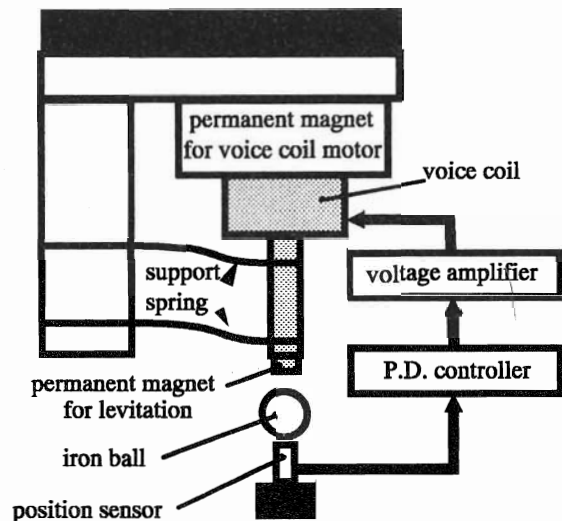


FIGURE 2: 1 DOF Magnetic Suspension System

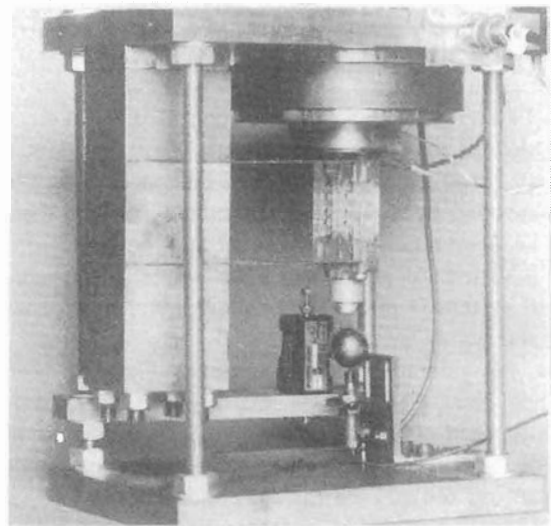


FIGURE 3: Photograph of Experimental Setup

$m_0$  = mass of the iron ball (0.0964 kg)  
 $m_1$  = mass of the shaded area in Figure 2 (0.0282 kg)  
 $R$  = resistance of the voice coil (6.35  $\Omega$ )  
 $L$  = inductance of the voice coil (5 mH)  
 $k_f$  = propulsive force constant (33.5 N/A)  
 $z_0$  = position of the iron ball (system output)  
 $z_1$  = position of the permanent magnet  
 $f_a$  = generating force by the VCM  
 $i$  = current of the voice coil  
 $V$  = applied voltage (system input)  
 $f_m$  = attractive force of permanent magnet.  
 The direction of the coordinate frame axis is downward.

### Theoretical Analysis

We investigate the feasibility of the proposed suspension system from linear control theory. The controllability and the observability of the experimental system are

checked. The stability of PD compensator and self-sensing system are examined.

**State Space Model** The equations of the motion of the ball and the magnet are

$$m_0 \ddot{z}_0 = m_0 g - f_m \quad (1)$$

$$m_1 \ddot{z}_1 + \xi \dot{z}_1 + k_c z_1 = f_a + f_m + m_1 g$$

The equations of the VCM are

$$L \dot{i} + R i + k_t \dot{z}_1 = V \quad (2)$$

$$f_a = k_i i$$

The attractive force  $f_m$  is represented as a nonlinear function of the length of the air gap and it becomes larger as the gap decreases. By linearization of this function around the equilibrium position, we obtain

$$-\frac{\partial f_m}{\partial z_0} = \frac{\partial f_m}{\partial z_1} = k_m, (k_m > 0) \quad (3)$$

We assume the state vector as  $x' = (z_0 \ z_1 \ \dot{z}_0 \ \dot{z}_1 \ i)$  and output  $y = z_0$ . From Equations (1), (2) and (3), the state space model is represented as

$$\dot{x} = Ax + bu \quad (4)$$

$$y = cx$$

**Controllability and Observability** The determinant of the controllability matrix of the system of Equation (4) is

$$\det(b \ Ab \ A^2 b \ A^3 b \ A^4 b) = -\frac{k_m^2 k_t^4}{L^5 m_0^2 m_1^4} \quad (5)$$

and the determinant of the observability matrix is

$$\det(c' \ (cA)' \ (cA^2)' \ (cA^3)' \ (cA^4)') = \frac{k_m^3 k_t}{m_0^3 m_1} \quad (6)$$

As Equations (5) and (6) are non-zero, the experimental system is controllable and observable and the feasibility of the proposed suspension system is verified.

**Stability of System with PD Compensator** Next, we examine the stability of the system with PD feedback scheme. The system is represented as the autonomy system

$$\dot{x} = (A - bk_{PD} C_{PD})x = A_{PD}x \quad (7)$$

where,

$$k_{PD} = (k_p \ k_d),$$

$$C_{PD} = \begin{pmatrix} 1 & 0 & 0 & 0 & 0 \\ 0 & 0 & 1 & 0 & 0 \end{pmatrix},$$

and  $k_p$  is a proportional gain and  $k_d$  is a differential gain. If the PD gains were brought to appropriate values, the roots of the determinant of  $(sI - A_{PD})$  could lie in the left half-plane. So, we can make the system stable with PD control. The gains which make the system stable are given later.

**Self-Sensing System** As the study of the system employing a self-sensing controller, which drives the voltage of the VCM and senses the current, we consider the following output equation.

$$y = c_s x = (0 \ 0 \ 0 \ 0 \ 1)x \quad (8)$$

The determinant of the observability matrix of this system is

$$\det(c_s' (c_s A)' (c_s A^2)' (c_s A^3)' (c_s A^4)') = \frac{k_c k_m^3 k_t^4}{L^4 m_{01}^3} \quad (9)$$

Equation (9) shows the probability of self-sensing controller. However, as the spring constant  $k_c$  is invoked in the right side of the equation, the permanent magnet must be supported by elastic element.

### Comparison of Experimental and Numerical Examination

On experimental examination of the system shown in Figure 3, it was verified that the iron ball can be suspended without any mechanical contact, with a precision better than 1  $\mu\text{m}$  which is as good as the sensor resolution.

**Step Response** The responses of the numerical simulation and the experiment to 0.1 mm step movement of the ball in the downwards direction were observed. The results are shown in Figure 4. To actuate the step movement of the ball, the magnet was initially moved upwards, thus decreasing the attractive force acting on

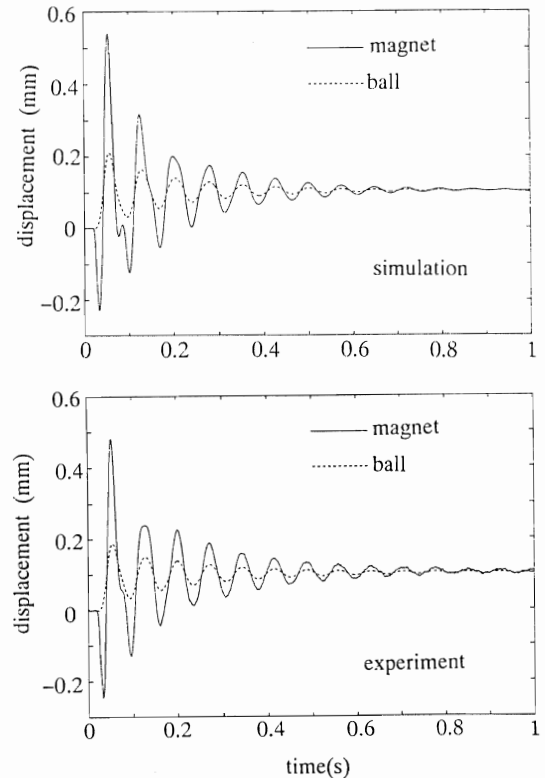


FIGURE 4: Step Response

the ball and allowing it to drop. Correct servo action of the system was then observed as the ball's position converged towards the new desired reference point. In addition, the ranges of feedback gains which provide stable suspension were investigated and the results compared well with numerical computations, thus giving credence to the theoretical analyses.

**Feedback Gains for Stable System** We investigate the feedback gains which make the suspension system stable. The theoretical range is calculated from Equation (7) using the Routh-Hurwitz stability criterion. In experiment, when differential gain was fixed to some values, the maximum and minimum values of stable proportional gain are measured. The result is shown in Figure 5. The region surrounded with a horizontal line and a slanted parabola is the theoretical stability range. Vertical lines show the experimental stability ranges. Both the upper and lower points of each line agree well with the range of theoretical calculation. This result confirms that the theoretical analysis can be used to verify the effectiveness of the application of various control systems.

### 3 DOF SUSPENSION SYSTEM

We have made a disk suspension system which has three above-mentioned mag-lev mechanisms. The structure is shown in Figure 6. The system uses a DSP (TMS320C31) as a digital controller. The movements of three magnets and 3 DOF of the disk which is a suspended object are sensed by 6 gap sensors. DSP controller calculates appropriate currents of motor based on the sensor signals converted by A/D converter and drives the motor through D/A converters and DC current amplifiers.

The photograph of experimental setup is shown in Figure 7. The permanent magnets are supported by ball bearings and are driven by VCMs. The center of this system is the center of the three axes of motors. The suspended disk is an iron plate with 3.2 mm thickness and 100 mm diameter. The magnets are ring-shapes with heights of 4.5 mm, inside diameters of 8 mm, and outside diameters of 20 mm. The coordinate frame is set with the z axis in the vertical direction and the y axis in the direction from left to right.

Two translational DOFs in horizontal plane and a rotation about z axis are not actively controlled. They are stabilized passively by the attractive forces on three iron ball halves which are located on the disk and under three permanent magnets, respectively.

### Parameters and Variables

Parameters and variables for the theoretical analyses are as follows. They are different from those of 1 DOF system model, even if same symbol. Subscript  $i$  indicates the position of a motor or a sensor shown in Fig-

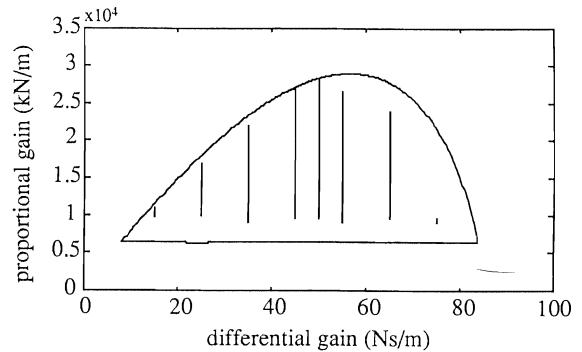


FIGURE 5: Stable PD Gains of the System

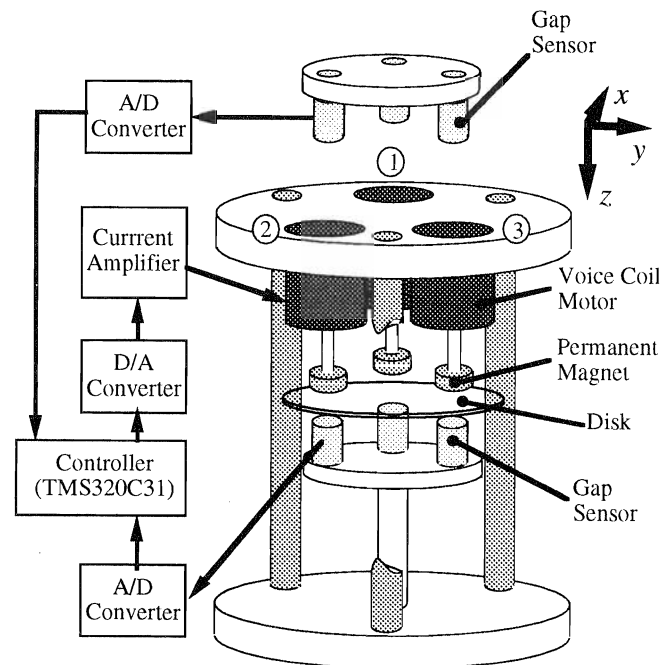


FIGURE 6: Structure of 3 DOF Suspension System

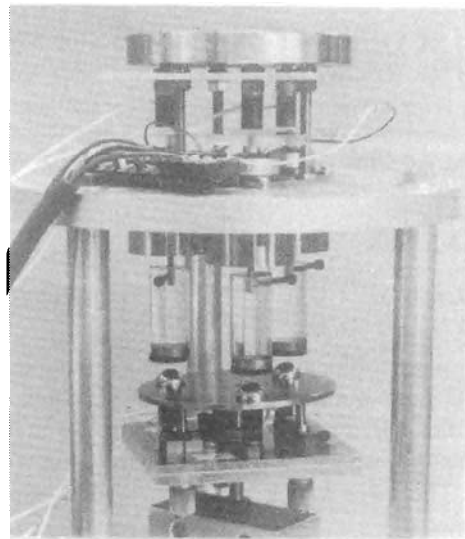


FIGURE 7: Photograph of Experimental Setup

ure 6, where  $i = 1, 2, 3$ .

- $m_0$  = mass of disk ( 0.220 kg )
- $I_q$  = inertia of disk about x or y axis (  $1.38 \times 10^{-4}$  kgm<sup>2</sup> )
- $m_i$  = mass of the part with a magnet ( 0.075 kg )
- $k_i$  = propulsive force constant ( 4.5 N/A )
- $r_m$  = distance from magnet to center ( 0.035 m )
- $r_s$  = distance from sensor to center ( 0.035 m )
- $z_0$  = vertical position of the suspended disk
- $q_x, q_y$  = rotation of the disk about x and y axis
- $z_i$  = position of a permanent magnet
- $s_i$  = sensor output for the disk
- $f_{mi}$  = attractive force of magnet
- $f_i$  = force of VCM
- $i_i$  = current of VCM ( system input )
- $d_i$  = air gap between magnet and disk

### Theoretical Analysis

We assume that the air resistance and the friction of motor bearing can be neglected, the center of gravity of the disk is aligned to the center of the system, and the characteristics of the permanent magnets are same. The equations of the motion of the disk are

$$m_0 \ddot{z}_0 = m_0 g - f_{m1} - f_{m2} - f_{m3}$$

$$I_\theta \ddot{\theta}_x = \frac{\sqrt{3}}{2} r_m (f_{m2} - f_{m3}) \quad (10)$$

$$I_\theta \ddot{\theta}_y = r_m f_{m1} - \frac{1}{2} r_m (f_{m2} + f_{m3})$$

The equations of the movement of the permanent magnets are

$$m_i \ddot{z}_i = m_i g + f_{mi} + f_i \quad (11)$$

The attractive forces of magnets are linearized as

$$f_{mi} = k_m (z_i - s_i) \quad (12)$$

The propulsive forces are proportional to the currents of voice coils.

$$f_i = k_i i_i \quad (13)$$

If the movement of disk is enough small, the relation between the sensor outputs and the movements of the disk is represented by

$$\begin{pmatrix} s_1 \\ s_2 \\ s_3 \end{pmatrix} = \begin{pmatrix} 1 & 0 & -r_s \\ 1 - \frac{\sqrt{3}}{2} r_s & \frac{1}{2} r_s & \\ 1 & \frac{\sqrt{3}}{2} r_s & \frac{1}{2} r_s \end{pmatrix} \begin{pmatrix} z_0 \\ \theta_x \\ \theta_y \end{pmatrix} = T_s \begin{pmatrix} z_0 \\ \theta_x \\ \theta_y \end{pmatrix} \quad (14)$$

The state vector is set to

$$x' = (z_0 \ \theta_x \ \theta_y \ z_1 \ z_2 \ z_3 \ \dot{z}_0 \ \dot{\theta}_x \ \dot{\theta}_y \ \dot{z}_1 \ \dot{z}_2 \ \dot{z}_3)$$

and the input vector and the output vector are

$$u' = (i_1 \ i_2 \ i_3), \quad y' = (s_1 \ s_2 \ s_3 \ z_1 \ z_2 \ z_3).$$

The state space model of this 3 DOF suspension system is represented by

$$\dot{x} = Ax + Bu \quad (15)$$

$$y = Cx$$

The system of Equation (15) is controllable and observable.

### Design of Controller

In this system, the axis of a VCM is aligned to the axis of a disk sensor. Two control methods are considered. One is a concentrated control system which controls a current of a VCM by all information from 6 sensors. The other is a decentralized control system which controls a current of a VCM by the information of only the two sensors on the axis of the VCM.

The system divides into three sub-systems. The state vector of a sub-system is  $x_d' = (s_i \ x_i \ \dot{s}_i \ \dot{z}_i)$ , the output vector and the input are  $y_d' = (s_i \ z_i)$ ,  $u_d = i_i$ . The state space model is

$$\dot{x}_d = \begin{pmatrix} \mathbf{0}_2 & \mathbf{I}_2 \\ k_m/m_d & -k_m/m_d \\ -k_m/m_i & k_m/m_i \end{pmatrix} x_d + \begin{pmatrix} \mathbf{0}_{3 \times 1} \\ k_i/m_i \end{pmatrix} u_d \quad (16)$$

$$y_d = (\mathbf{I}_2 \ \mathbf{0}_2) x_d$$

where,  $m_d = m_d/3$ .

Using PD control method, the system has state feedback loop. The feedback gains are calculated by optimal regulator theory. Three types of gains are calculated.

1) decentralized control, attention to  $y_d$  and  $u_d$

2) concentrated control, attention to  $y$  and  $u$

3) concentrated control, attention to  $x$  and  $u$

The gains of Methods 1) and 2) are obtained such as the next cost functional is minimized.

$$J = \int_0^\infty (y' P y + u' R u) dt \quad (17)$$

Method 3) uses the next functional.

$$J = \int_0^\infty (x' Q x + u' R u) dt \quad (18)$$

Matrices P, Q, and R are

1) P = diag(100 100), R = 1,

2) P = diag(100 100 100 100 100 100), R = diag(1 1 1),

3) Q = diag(100 10 10 100 100 100 0 0 0 0 0), R = diag(1 1 1).

The state feedback gain matrix can be transformed to the sensor signal feedback gain matrix by linear coordinate transformation. The sensor feedback gain matrices which are obtained from Methods 1), 2) and 3) are all grouped into the next equation.

$$K = \begin{pmatrix} a_1 & b_1 & b_1 & a_2 & b_2 & b_2 & a_3 & b_3 & b_3 & a_4 & b_4 & b_4 \\ b_1 & a_1 & b_1 & b_2 & a_2 & b_2 & b_3 & a_3 & b_3 & b_4 & a_4 & b_4 \\ b_1 & b_1 & a_1 & b_2 & b_2 & a_2 & b_3 & b_3 & a_3 & b_4 & b_4 & a_4 \end{pmatrix} \quad (19)$$

The gains of three controllers are shown in Table 1. From the table, we can find that the gains of Methods 1) and 2) are very similar. It shows that if we use optimal regulator theory with attention to outputs and inputs,

Table 1 Optimal Feedback Gains

	$a_1$	$a_2$	$a_3$	$a_4$	$b_1$	$b_2$	$b_3$	$b_4$
1)	-151	137	-3.68	2.13	0	0	0	0
2)	-150	135	-3.67	2.12	-0.52	0.52	0	0
3)	-234	180	-5.92	2.44	45.4	-24.4	1.23	-0.17

the concentrated controller is not better than the decentralized one.

**Numerical Simulation**

We make a numerical simulation to examine the control performance of above 3 methods. The simulation is based on the linear model of Equation (15). The initial position of magnet 1 is 0.5 mm downward from equilibrium position. The movement of disk and input currents are recorded until the system converges on the equilibrium position.

The results are shown in Figure 8. Responses of Methods 1) and 2) are similar. In the system of Method 3), the errors of gradients of the disk converge more quickly than the  $z_0$  movement. From the figures of currents, we can see that system does not drive only the VCM 1 but VCM 2 and 3.

If the suspended disk has not the iron ball halves, the system must control the translational motion in the horizontal plane. It is important to control the gradient of the disk, which actuates in the horizontal direction in this case. Method 3) is useful.

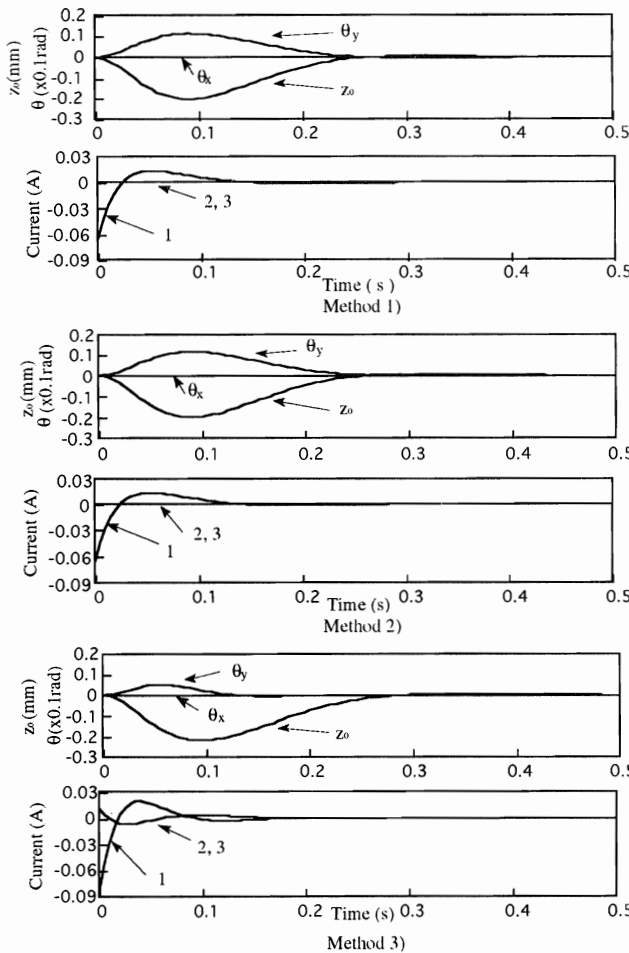


**FIGURE 8: Simulation Results**

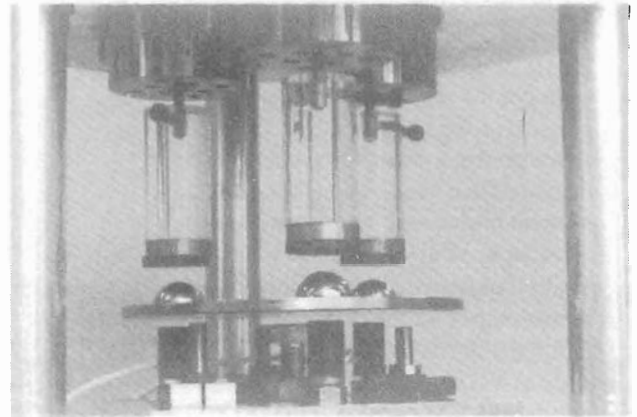


**FIGURE 9: Photograph of Suspended Disk**

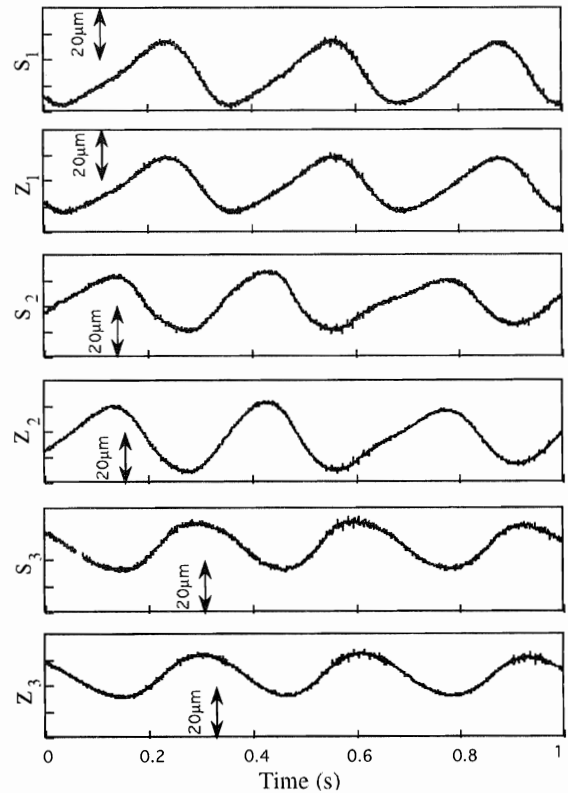


**FIGURE 10: Sensor Signals During Suspension**

**Experimental Examination**

Suspension examination of the system shown in Figure 7 is carried out. A photograph in the state of suspension is shown in Figure 9. The sensor signals during suspension are recorded in Figure 10. The control method is decentralized system. The gains  $a_1, a_2, a_3, a_4$  in Equation (17) are -886, 750, -26, 11, respectively. The reasons for the differences are to account for the velocity term of weight matrix in optimal regulator theory and to make the system robust.

Sensor signals have residual vibration with peak to peak 20 or 30  $\mu\text{m}$ . The vibration is caused by the weakness

of centripetal force in the horizontal direction, because the shape of the magnet is a ring. This problem can be solve by using small diameter magnets.

**FURTHER SYSTEM**

With the proposed concept of controlling force by varying the air gap length, we can consider various interesting levitation systems. We introduce two possible levitation systems.

**Mag-lev System with Piezoelectric Element and Permanent Magnet**

A system employing a piezoelectric actuation element and self-sensing controller has been considered. By nature, piezoelectric elements incorporate both drive and support mechanisms, permitting designs that are both simple and small-scale. It follows that by simply attaching a permanent magnet to the tip of a piezo element, a levitation system can be made.

The outline of the system is shown in Figure 11. The equivalent circuit model is shown in Figure 12. Considering the characteristics of the equivalent circuit, we can represent the system as

$$\begin{aligned}
 m_0 \ddot{x}_0 &= f_m \\
 m_1 \ddot{x}_1 &= TV - f_m - R_d \dot{x}_1 - x_1 \\
 c_d \dot{V} &= i - T \dot{x}_1
 \end{aligned}
 \tag{20}$$

The state space mode from Equation (20) which input is the current of piezoelectric element and output is the voltage, is controllable and observable.

**Application of Electrostatic Suspension System**

The concept of using electrostatics, in place of permanent magnets, as an attractive force means is introduced. The structure of the system is shown in Figure 13. As the first step of the electrostatic suspension system without mechanical contact, the suspended disk, made of silicon is supported by a spring. In this system, we can verify the feasibility of electrostatic suspension on experiment.

**CONCLUSION**

A novel active mag-lev system, featuring a bearing force control method, was proposed. In the proposed system, bearing force is controlled by a mechanical method in which the air gap between a permanent magnet and suspended object is varied by an actuator.

A 1 DOF experimental system is made and analyzed theoretically. On experimental examinations, it was verified that the iron ball can be suspended without any mechanical contact and the theoretical analysis was supported well.

A 3 DOF disk suspension system is introduced. Three types of controllers for the system are examined by numerical simulation.

As further application, two interesting levitation sys-

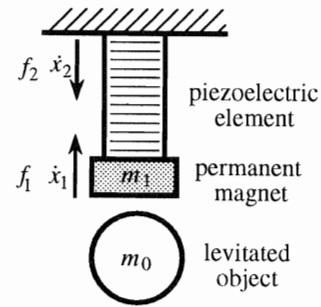


FIGURE 11: Outline of Simple Suspension System with Piezoelectric Element

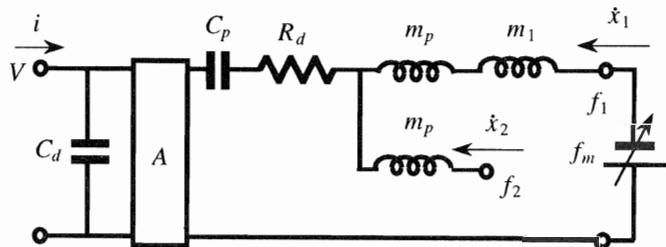


FIGURE 12: Equivalent Circuit of Piezoelectric Suspension System

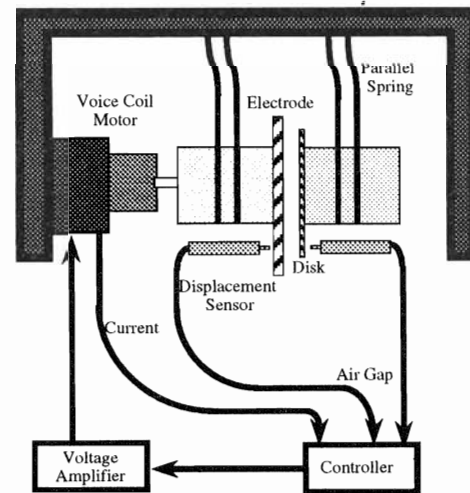


FIGURE 13: Electrostatic Suspension System

tems are proposed.

**ACKNOWLEDGMENT**

The authors would like to thank Mr. Allan Kelly for his improvement of the composition of this paper. This work was in part based on the research project of the Grant-in-Aid for Scientific Research (05750234)

**REFERENCES**

1. Jayawant B.V., Electromagnetic Levitation and Suspension Techniques, Edward Arnold, 1981
2. Bleuler H., A Survey of Magnetic Levitation and Magnetic Bearing Types, JSME Int. J. III Vol. 35-3, 335-342, 1992

